

Phone Tracking in Homogeneous Magnetic Field

Yan Yan

Department of Biomedical Engineering
University of Basel, Switzerland
yan.yan@students.fhnw.ch

Abstract—In biomedical engineering, precise positioning technology is critical for surgical navigation, implant monitoring, and the development of smart medical devices. This study investigates the calibration and tracking of a smartphone's built-in Hall effect sensor within a homogeneous magnetic field generated by Helmholtz air coils. By utilizing a pre-generated magnetic field lookup table, the system enables accurate tracking. Through a detailed exploration of the experimental setup, sensor calibration, lookup table generation, and position tracking, this study highlights the effectiveness of smartphone magnetometers in tracking applications.

Keywords—Smartphone Magnetometer, Helmholtz Coil, Sensor Calibration, PCB Technology, Magnetic tracking.

I. INTRODUCTION

In biomedical engineering, precise positioning technology is essential for applications like surgical navigation, implanted device monitoring, and the development of smart medical devices [1]. However, traditional positioning methods, such as optical or ultrasonic tracking, often face challenges like line-of-sight dependency and limited precision in complex environments. This highlights the need for alternative approaches, such as magnetic field-based positioning.

Magnetic field positioning offers a non-invasive, cost-effective solution. Smartphones, with their widespread availability and built-in sensors, have the potential to become powerful tools for precise medical applications, from guiding surgical tools to tracking miniaturized devices in vivo.

This study investigates an approach to tracking biomedical instruments (using smartphone sensors as substitutes) by using a high-precision magnetic field lookup table, combined with quadrilateral measurements, to locate a smartphone's magnetic field sensor. A Helmholtz coil is utilized to create a uniform magnetic field, ensuring accuracy and consistency in sensor readings.

II. METHOD

A. Calibration of Smartphone Magnetometer using a Helmholtz Coil

1) Generating a Homogeneous Magnetic Field

For magnetometer calibration, a homogeneous magnetic field provides a stable, interference-free environment that ensures accurate, consistent, and reproducible calibration of phone sensors, which is critical for their effective use in precision applications like biomedical device tracking or navigation systems.

There are two common configurations: the Helmholtz coils and the Maxwell coils. In this experiment, we chose the Helmholtz configuration (Fig. 1), which uses two identical coils of radius R , positioned at a distance equal to their radius

R . The magnetic field of each individual coil is non-uniform. Upon superimposition of the two fields, a central region with a magnetic field that is largely uniform is created between the two coils (Fig. 2), aiding in the precise localization of the smartphone. In contrast, Maxwell configuration produces a gradient magnetic field with zero field strength at the center, which is commonly used in MRI applications. Due to the gradient magnetic field, the magnetometer is applied with a magnetic force, which is not suitable for statics precise calibration.

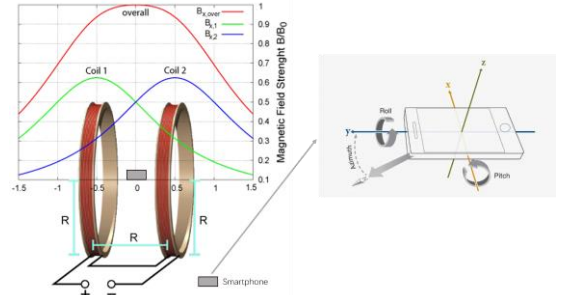


Fig. 1: Helmholtz coil

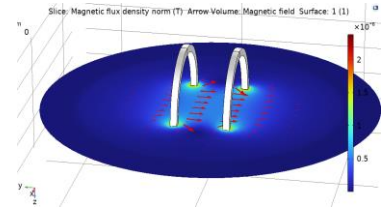


Fig. 2: The homogeneous Magnetic Field at the center [2]

2) Calibration Setup

The smartphone (represented by the gray box in Fig. 1) was positioned at the center of the Helmholtz coils. To collect magnetic field data, the Phyphox app was utilized. A DC power supply was used to provide a controlled voltage, generating a small, unidirectional current through both coils. The voltage and current levels were continuously monitored using a multimeter to ensure accuracy and stability during the experiment.

To calibrate the magnetometer, voltages of 1 V and 2 V were applied to the Helmholtz coil, producing currents of 0.4335 A and 0.8561 A, respectively. This configuration generated the primary magnetic field along the Y-axis of the smartphone's coordinate system, aligned through the centers of both coils (Fig. 1). To assess the impact of magnetic hysteresis, the current direction was reversed, altering the orientation of the magnetic field.

3) Data Processing Steps

The collected data was then processed using MATLAB. The processing steps included offset removal, noise filtering to minimize interference, and the estimation of the sensor's resolution and sensitivity.

B. Coil Design on Printed Circuit Board (PCB)

1) Quadrilateration

We plan to utilize quadrilateration for localization instead of trilateration (Fig. 3a). This approach involves an arrangement of four coils in a two-by-two array (Fig. 3b). The use of four coils offers an additional reference point, which not only extends the tracking range to $40\text{ mm} \times 40\text{ mm} \times 40\text{ mm}$ but also enhances positioning accuracy, making it more effective for precise localization.

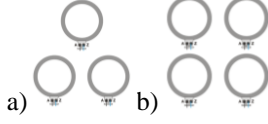


Fig. 3: a) Coils of Trilateration; b) Coils of quadrilateration.

2) Air Core Coils

We opted to design an air-core coil due to its linear behavior and simplicity in modeling. Unlike ferromagnetic core coils, air-core coils offer significant advantages: they do not experience magnetic saturation, are free from magnetic hysteresis, exhibit no dependency on temperature variations and avoid field lines deviation between the multiple coils. These characteristics make air-core coils ideal for generating consistent and predictable magnetic fields, which are crucial for accurate experimental results.

3) Design Coils on Printed Circuit Board

To obtain a lightweight magnetic field generator we will manufacture the coils in a Printed Circuit Board, PCB. The standard PCB technology requires to follow the following design rules:

- Number of Layers (NL): 4
- Track Width (Wd): $902\text{ }\mu\text{m}$
- Track Thickness ($T_{thickness}$): $140\text{ }\mu\text{m}$
- Minimal spacing between the tracks: $330\text{ }\mu\text{m}$
- Number of Turns per Layers (N): 74

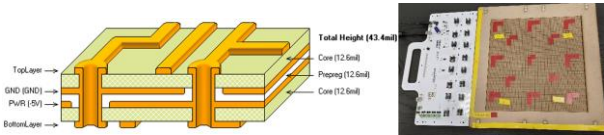


Fig. 4: (Left) Example of Four-layer PCB (cross section) from [3]. (The dimensions are indicative and do not correspond to our manufacturer); (Right) Magnetic Experimental Device for Smartphone Positioning

As the PCB corresponds to a stack of planar structures (Fig. 4 Left), we will design the coils with a spiral geometry. Each of the four coils corresponds to a series connection of four coils manufactured on each of the four layers of the PCB, which can increase the magnetic strength and uniformity.

To ensure a sufficient tracking volume above the magnetic field generator, the outer diameter of the coil shall be $Do = 195.5\text{ mm}$. To ensure the possibility to connect the four coils located on each of the four PCB layers, the inner diameter of the coil shall be $Di = 6.6\text{ mm}$. To limit the power dissipation, the maximal current injected through each spiral coil shall be 2 A DC .

The final experimental setup is shown in Fig. 4 Right.

C. Phone Tracking in Magnetic Fields

To implement quadrilateration for phone positioning, each coil was activated sequentially, starting with *Coil A* and progressing through *Coil D*. Afterward, an offset measurement was conducted with all coils deactivated to establish the baseline magnetic field. The magnetic field strengths of the four coils were recorded during this process, along with the corresponding measurements, to facilitate accurate positioning. We repeat the entire measurement process multiple times to reduce noise errors by averaging the results.

By comparing the magnetic field strengths at the smartphone's location relative to each coil with the corresponding reference values from a pre-calculated lookup table — generated based on the coils' design specifications and characteristics — quadrilateration is employed to accurately determine the smartphone's coordinates $[x, y, z]$ within the defined space.

III. RESULTS

A. Smartphone Magnetometer Calibration

1) Reference Magnetic Field Strength Calculation

To calculate the theoretical magnetic field (or magnetic flux density) B_{ref} generated in the center of the Helmholtz coil at the current $I\text{ A}$, we can use the following formula:

$$B_{ref} = \mu_0 \cdot \frac{8 \cdot I \cdot N}{\sqrt{125} \cdot R} \quad (1)$$

Where μ_0 is the vacuum permeability, its value equals to $4\pi \times 10^{-7}\text{ H/m}$, I = coil current, R is radius and distance of coils.

For this Helmholtz pair of coils, we get:

$$B_{ref} = 743.3 \times I \text{ in } \mu\text{T} \quad (I \text{ in A}) \quad (1^*)$$

When $I = 1\text{ A}$, $B_{ref} = 743.3\text{ }\mu\text{T}$. The maximum magnetic field strength at 5 A is $B_{max} = 3716.5\text{ }\mu\text{T}$ [4].

Using formula (1) or (1*), we calculated the theoretical magnetic field strength B_{ref} corresponding to the currents applied during sensor calibration. The results are presented in Table 1 below.

Current $I\text{ (A)}$	$B_{ref}\text{ (}\mu\text{T)}$
0.4335	322.2206
0.8561	636.3391
-0.4335	-322.2206
-0.8561	-636.3391

Table 1: Magnetic Strength Reference at Positive and Negative Currents

2) Data Processing

We used MATLAB to process the data acquired from the Phyphox app on the smartphone. First, we visualized the raw data, revealing offsets in each direction when the current was switched off. To address this, we subtracted the offsets caused by Earth's magnetic field and environmental interference from the raw data to obtain the calibrated data. A moving average filter was then applied to reduce noise influence. The results show that the homogeneous magnetic field generated by the Helmholtz coils primarily aligns with the smartphone's Y-axis, as indicated by the prominent plateau phase.

The mean calibrated magnetic field strengths along the Y-axis during the plateau phase under different currents are summarized in Table 2 below.

Current I (A)	$B_{y_measured}$ (μT)
0.4335	324.7157
0.8561	644.0093
-0.4335	-323.7873
-0.8561	-606.4449

Table 2: Magnetic Strength Measurement at Positive and Negative Current

3) Linear correlation

The fitting line of $B_{y_measured}$ against B_{ref} (Fig. 5) reveals a positive linear relationship, indicating that the sensor's response to the magnetic field is highly linear. The calculated correlation coefficient (R) is 0.9997, and the coefficient of determination (R^2) is 0.9994. These results demonstrate a strong correlation, confirming the success of the calibration process and the sensor's ability to accurately respond to changes in the magnetic field.

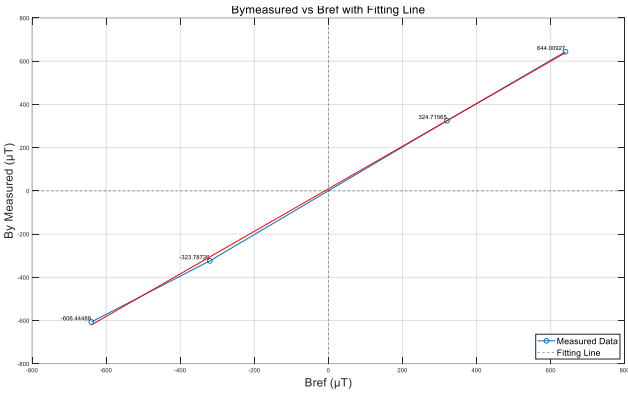


Fig. 5: Measured Magnetic Strength vs Reference Magnetic Strength with Fitting Line

4) Sensitivity and Resolution

We use the following formula to calculate the estimated sensitivity error (ESE):

$$ESE = \frac{|B_{y_measured} - B_{ref}|}{B_{ref}} \times 100\%$$

The ESE results for the corresponding currents are presented in Table 3. The overall estimated sensitivity errors are minimal, indicating that the calibration process is highly reliable.

Current I (A)	Estimated Sensitivity Error (ESE)
0.4335	1.40%
0.8561	1.21%
-0.4335	1.11%
-0.8561	4.70%

Table 3: Estimated Sensitivity Errors under Different Currents

The standard deviations under different currents were calculated and are presented in Table 4. The original curve, along with the curve adjusted by plus and minus one standard deviation ($Current = 0.4335 A$), is shown in Fig. 6. This demonstrates that the instrument reliably captures signal changes beyond the noise level. The resolution is defined by the standard deviation, and the calibrated signal meets the experimental requirements.

Current I (A)	Standard Deviation
0.4335	0.3235
0.8561	0.5265

-0.4335	0.3475
-0.8561	0.4314

Table 4: Standard Deviations under Different Currents

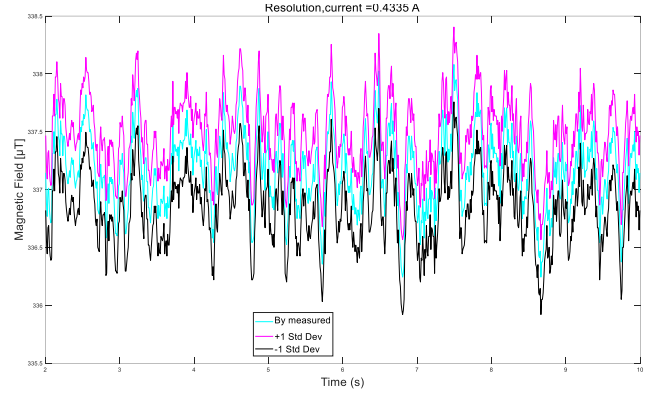


Fig. 6: Sensor Resolution

B. Phone Position Calculation in Magnetic Fields

The following Table 5 is a summary of the calculated necessary parameters for the spiral coils on PCB.

Coil Properties	Value
Magnetic Flux Density at the Center of the Spiral Coil	$B = 0.0133 T$
Effective Cross Section	$A = 37.3789 mm^2$
Length of Section	$L = 94.45 mm$
Height of the Coil	$H_{coil} = 0.396 mm$
Current Density	$J_{coil} = 15.838 A/mm^2$

Table 5: Parameters important for PCB Magnetic Field Simulation

Using these parameters, we can simulate the magnetic fields generated by the four coils (using Python or Wolfram). Based on the simulation, the magnetic field strength of each coil at various positions is calculated to construct the lookup table. The magnetic field strength at each position is measured five times: once with no coil activated to measure the offset and four times with each coil (A, B, C, and D) activated successively to measure the magnetic field generated by each coil along with the offset. We applied the previous calibration process to obtain the pure offset and the magnetic field strength of each coil at the phone's position along the X, Y, and Z axes (Fig. 7).

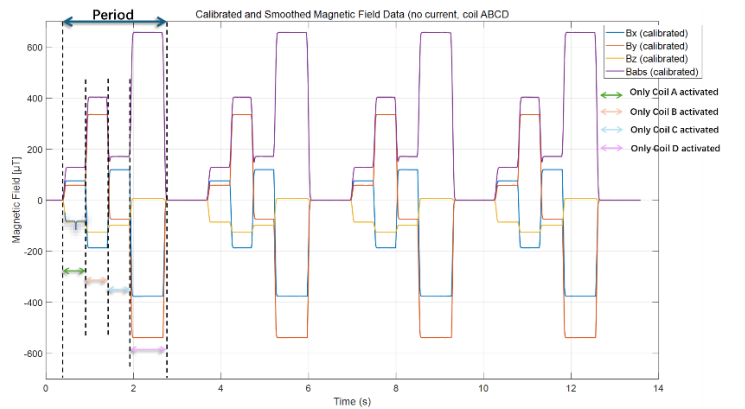


Fig. 7 Smoothed and Calibrated Magnetic Field Data.

The calculated magnetic strength of each coil at phone position is shown below (unit: μT):

$$B_A = [75.0787 \quad 57.9764 \quad -84.8120]$$

$$B_B = [-186.4059 \quad 335.4354 \quad -125.3279]$$

$$B_C = [119.7497 \quad -73.6566 \quad -97.6628]$$

$$B_D = [-376.2632 \quad -538.2038 \quad 6.7634]$$

Using quadrilateration, we minimize the norm of the relative distance (Fig. 8) between the measured magnetic field strengths from the sensor and the corresponding values in the lookup table. The point X at which this function is minimized represents the calculated location.

$$f(X') = \left\| \begin{array}{c} B_A(X) - B_A'(X') \\ B_B(X) - B_B'(X') \\ B_C(X) - B_C'(X') \\ B_D(X) - B_D'(X') \end{array} \right\|_2$$

Fig. 8: Formula of Norm of Relative Distance. $B_i(X)$, where $i = A, B, C, D$, is the measured absolute magnetic strength of each coil at position X , where $X = [x, y, z]$; $B_i'(X')$, where $i = A, B, C, D$, is the simulated absolute reference magnetic strength of each coil at position X' , where $X' = [x, y, z]$.

The provided MATLAB code was utilized to compute the smartphone's position. The calculated result and its visualization (Fig. 9) are shown below:

$$X = [10 \quad 30 \quad 3]$$

Since the lookup table is discrete, we accept a positioning error with a maximum of half the distance between two adjacent points. In our case, the maximum error is 2.5 mm.

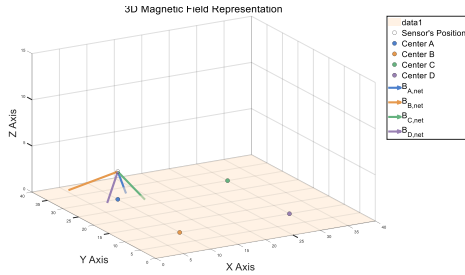


Fig. 9: Visualization of Smartphone Position

IV. DISCUSSION

We observe a slightly larger difference between the magnetic field generated by a current of $I = -0.8561 \text{ A}$ and its reverse current compared to the difference observed at $I = -0.4335 \text{ A}$ and its reverse current (Table 2). Additionally, the estimated sensitivity error is relatively higher under $I = -0.8561 \text{ A}$ (Table 3). Furthermore, the standard deviation increases as the current rises from $|I| = 0.4335 \text{ A}$ to 0.8561 A (Table 4). As shown in Fig. 10, the magnetic field strength in the X and Z axes shows very small residual values. These findings indicate that while the system can accurately locate the mobile phone to a certain extent, there are still some limitations and challenges that need to be addressed to further improve accuracy.

1) Smartphone Position:

The phone is placed in magnetic field manually, so the Y axis of phone may not strictly align with the center axis of Helmholtz coils. Additionally, due to the protrusion of the camera on the back of the smartphone, the phone could not lie completely flat on the four-coil setup, resulting in a height offset along the Z-axis.

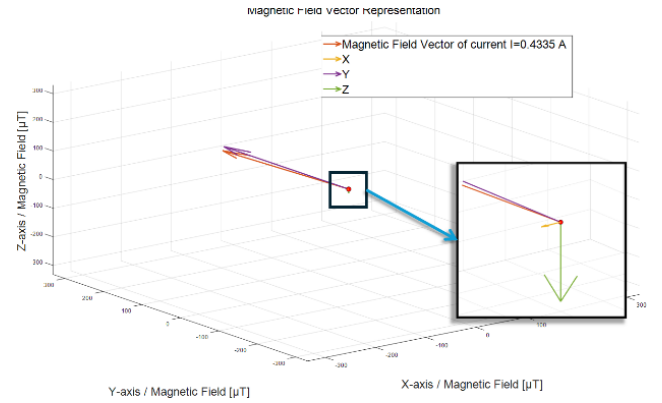


Fig. 10: Small Residual in X and Z Axis (current = 0.4335 A)

2) Magnetic Hysteresis:

The phone sensor material may retain some magnetic remanence, even when the external magnetic field is zero, reducing tracking accuracy.

3) Environmental Magnetic Field Fluctuations:

Background magnetic fields may vary due to electromagnetism interference, such as equipment turning on/off or power noise.

4) Sensor Drift:

Magnetometer readings can shift due to temperature changes or other operational conditions.

5) Use of Voltage Source:

The experiment used a voltage source to provide constant voltage. However, a current source would be preferable as it ensures stable current input, reducing coil current fluctuations and providing a more consistent and predictable magnetic field.

6) Lookup Table's Discreteness:

The lookup table's discreteness can introduce errors, which can be mitigated using interpolation. Interpolation creates a continuous volumetric model from discrete points, providing more spatial coverage and enabling more accurate estimation of magnetic field strengths at intermediate points, thereby reducing resolution-related errors.

V. CONCLUSION

This study highlights the potential of using smartphone magnetometers for precise positioning within the magnetic field generated by Helmholtz coils. Calibration and processing ensure accurate tracking with strong linearity. Despite certain imperfections, the system is expected to have medical applications, including tracking surgical tools and monitoring implants, providing a cost-effective solution for precise healthcare positioning.

REFERENCES

- [1] Yang, R., Li, C., Tu, P., Ahmed, A., Ji, T., & Chen, X. (2022). Development and Application of Digital Maxillofacial Surgery System Based on Mixed Reality Technology. *Frontiers in Surgery*, 8. <https://doi.org/10.3389/fsurg.2021.719985>.
- [2] www.comsol.com/model/magnetic-field-of-a-helmholtz-coil-15
- [3] www.bitweenie.com/listings/pcb-layers/
- [4] www.3bscientific.com/product-manual/1000906.pdf